Yangian symmetry for fishnet Feynman graphs

Dmitry Chicherin, Vladimir Kazakov, Florian Loebbert, Dennis Müller, and De-liang Zhong

Yangian Symmetry for Fishnet Feynman Graphs

Dmitry Chicherin,[1, *] Vladimir Kazakov,[2, †] Florian Loebbert,[3, ‡] Dennis Müller,[3, §] and De-liang Zhong[2, ¶]

[1]*PRISMA Cluster of Excellence, Johannes Gutenberg University, 55099 Mainz, Germany*
[2]*Laboratoire de Physique Théorique, Département de Physique de l'ENS,*
Ecole Normale Supérieure, PSL Research University, Sorbonne Universités,
UPMC Univ. Paris 06, CNRS, 75005 Paris, France
[3]*Institut für Physik, Humboldt-Universiät zu Berlin,*
Zum Großen Windkanal 6, 12489 Berlin, Germany &
Kavli Institute for Theoretical Physics, University of California, Santa Barbara, CA 93106, USA
(Dated: September 19, 2017)

Various classes of fishnet Feynman graphs are shown to feature a Yangian symmetry over the conformal algebra. We explicitly discuss scalar graphs in three, four and six spacetime dimensions as well as the inclusion of fermions in four dimensions. The Yangian symmetry results in novel differential equations for these families of largely unsolved Feynman integrals. Notably, the considered fishnet graphs in three and four dimensions dominate the correlation functions and scattering amplitudes in specific double scaling limits of planar, γ-twisted $\mathcal{N} = 4$ super Yang–Mills or ABJM theory. Consequently, the study of fishnet graphs allows us to get deep insights into the integrability of the planar AdS/CFT correspondence.

INTRODUCTION

Feynman diagrams represent the main tool for the study of complex physical phenomena—from fundamental interactions of elementary particles to diverse solid state systems. In spite of the great progress in computing individual Feynman graphs with multiple loop integrations, examples of exact all-loop results for important physical quantities (such as amplitudes, correlators, etc.) are rare in dimensions greater than two. Remarkably, there exist certain types of planar graphs with a particularly regular structure, which may be calculable at any loop order. Examples are the regular tilings of the two-dimensional plane. These diagrams become accessible due to their integrability properties, in close analogy to the quantum integrable one-dimensional Heisenberg spin chains. Apart from providing new, powerful methods for the computation of large classes of particular Feynman graphs, these observations reveal the interplay between various physical systems and a rich variety of mathematical aspects related to quantum integrability.

A prime example in the above class of Feynman graphs are scalar fishnets in four dimensions, built from four-point vertices connected by massless propagators (cf. Fig. 1). These represent one of the three regular tilings of the Euclidean plane and, except for the simplest example, solving this class of Feynman integrals for generic external parameters is an open problem. On the other hand, these square fishnets are subject to outstanding properties: Firstly, they feature a (dual) conformal Lie algebra symmetry, which makes it natural to express them using conformal cross ratios. They are finite, i.e. free of IR or UV divergencies, such that their conformal symmetry is unbroken for generic kinematics. Moreover, A. Zamolodchikov demonstrated that scalar fishnet graphs can be interpreted as integrable vertex models [1]. Further-
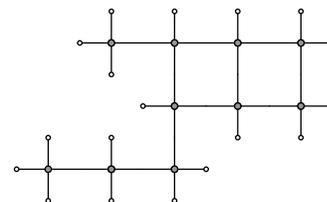
FIG. 1. Example of a conformal scalar fishnet Feynman graph in four dimensions. Filled blobs denote loop integrations, white blobs represent external points x_k.

more, in the planar limit fishnet graphs dominate physical quantities, such as scattering amplitudes and correlators, of the bi-scalar CFT recently found by Ö. Gürdogan and one of the authors [2] as a specific double-scaling limit of γ-twisted $\mathcal{N} = 4$ SYM theory. This non-unitary CFT is defined by the Lagrangian

$$\mathcal{L}_\phi = N_{\rm c} \operatorname{Tr}\big(\partial^\mu \phi_1^\dagger \partial_\mu \phi_1 + \partial^\mu \phi_2^\dagger \partial_\mu \phi_2 + \xi^2 \, \phi_1^\dagger \phi_2^\dagger \phi_1 \phi_2\big). \quad (1)$$

Its basic physical quantities (anomalous dimensions, correlators etc.) are determined by a very limited number of Feynman graphs at each loop order and efficiently calculable via integrability [3, 4].

In this letter we add a further remarkable property to the above list of features of fishnet graphs. We demonstrate that their conformal symmetry extends to a non-local Yangian symmetry. This symmetry yields novel differential constraint equations for this class of Feynman integrals. More technical details can be found in the accompanying papers [5, 6].

A single scalar fishnet graph of the above type represents a single-trace correlator of the bi-scalar theory:

$$K(x_1, \ldots, x_n) = \langle \operatorname{Tr}[\chi_1(x_1) \ldots \chi_n(x_n)] \rangle. \quad (2)$$
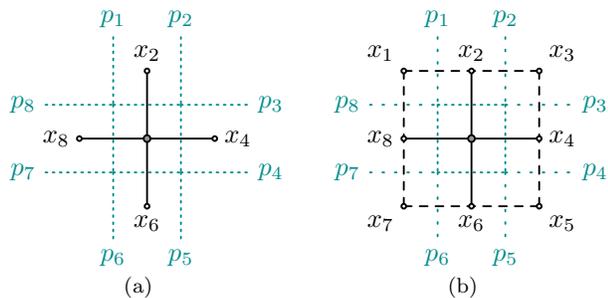
FIG. 2. The box integral in momentum (black) and dual (green) coordinate space. It will be convenient to distinguish (a) off-shell and (b) on-shell external momenta. Note the relabelling of coordinates with respect to (3).

Here $\chi_k \in \{\phi_1, \phi_2, \phi_1^\dagger, \phi_2^\dagger\}$ and x_i is the spacetime coordinate of the field χ_i. Importantly, via the relation to this bi-scalar model, we define a CFT for the all-loop study of Yangian-invariant correlators and scattering amplitudes, similar to those appearing in AdS/CFT. After having discussed the above scalar fishnets in four dimensions, we will show that the class of Yangian-invariant Feynman graphs is actually much richer and extends to different dimensions, particle species and more exotic tilings of the plane.

THE BOX AND THE YANGIAN

The most elementary representative in the class of fishnet graphs is the scalar box integral [7], cf. Fig. 2. In fact, this integral is the only member of this family, which has been solved explicitly. It is conveniently written in terms of variables x_i which can be related to dual momenta via $p_i^\mu = x_i^\mu - x_{i+1}^\mu$. The scalar box integral then reads

$$I_4 = \int \mathrm{d}^4 x_0 \frac{1}{x_{01}^2 x_{02}^2 x_{03}^2 x_{04}^2}, \qquad (3)$$

and evaluates to a combination of logs and dilogs of conformal cross ratios [8]. The above box integral (3)—as well as all fishnet graphs composed from such elementary boxes—are invariant under the conformal algebra $\mathfrak{so}(2,4)$. On a generic scalar fishnet graph, the conformal generators are represented via their usual tensor product representation $\mathrm{J}^A = \sum_{j=1}^n \mathrm{J}_j^A$ with the index j labeling the external legs and the index A enumerating the following differential operators:

$$\mathrm{D} = -ix_\mu \partial^\mu - i\Delta, \quad \mathrm{L}_{\mu\nu} = ix_\mu \partial_\nu - ix_\nu \partial_\mu + S_{\mu\nu}, \quad (4)$$
$$\mathrm{P}_\mu = -i\partial_\mu, \quad \mathrm{K}_\mu = 2x^\nu \mathrm{L}_{\nu\mu} - i(x^\nu x_\nu)\partial_{x^\mu} - 2i\Delta x_\mu.$$

As long as we consider only scalars, we have $S_{\mu\nu} = 0$.

The Yangian Hopf algebra over the conformal algebra is generated by the above Lie algebra generators and an additional set of bi-local level-one generators of the form

$$\widehat{\mathrm{J}}^A = f^A{}_{BC} \sum_{k=1}^n \sum_{j=1}^{k-1} \mathrm{J}_j^C \mathrm{J}_k^B + \sum_{j=1}^n v_j \mathrm{J}_j^A. \qquad (5)$$

Here $f^A{}_{BC}$ denotes the structure constants of the conformal algebra and the (a priori undetermined) variables v_j parametrize an external automorphism of the Yangian. The level-one generators obey the commutation relations $[\mathrm{J}^A, \widehat{\mathrm{J}}^B] = f^{AB}{}_C \widehat{\mathrm{J}}^C$.

The conformal algebra ensures the full Yangian symmetry, as soon as invariance under a single level-one generator and the full level-zero algebra holds. A convenient choice for demonstrating this invariance is the level-one momentum generator $\widehat{\mathrm{J}}^A \sim \widehat{\mathrm{P}}$ given by

$$\widehat{\mathrm{P}}^\mu = -\frac{i}{2} \sum_{j<k=1}^n \left[(\mathrm{L}_j^{\mu\nu} + \eta^{\mu\nu}\mathrm{D}_j)\mathrm{P}_{k,\nu} - (j \leftrightarrow k)\right] + \sum_{j=1}^n v_j \mathrm{P}_j^\mu. \qquad (6)$$

We may explicitly act with this generator onto the box integral (3) to find $\widehat{\mathrm{P}}^\mu I_4 = \sum_{j=1}^4 (v_j + j)\mathrm{P}_j^\mu I_4$. Hence, fixing the parameters v_j according to

$$v_j^{\mathrm{box}} := -j, \qquad (7)$$

the box integral is indeed Yangian-invariant. Parametrizing the box as $I_4 = \frac{1}{x_{13}^2 x_{24}^2}\Phi(u,v)$, with the conformal cross ratios $u = \frac{x_{12}^2 x_{34}^2}{x_{13}^2 x_{24}^2}$ and $v = \frac{x_{14}^2 x_{23}^2}{x_{13}^2 x_{24}^2}$, this statement boils down to the following second order differential equation,

$$0 = \Phi + (3u - 1)\frac{\partial \Phi}{\partial u} + 3v\frac{\partial \Phi}{\partial v} + (u-1)u\frac{\partial^2 \Phi}{\partial u^2}$$
$$+ v^2 \frac{\partial^2 \Phi}{\partial v^2} + 2uv\frac{\partial^2 \Phi}{\partial u \partial v}, \qquad (8)$$

as well as the same equation with u and v interchanged.

Notably, the above box integral has a cyclic shift symmetry $x_k \to x_{k+1}$. For $v_j = 0$ with $j = 1, \ldots, 4$, this symmetry is violated by the level-one generators in (5). Crucially, the choice of parameters (7) precisely restores this cyclic symmetry. In the case of the Yangian symmetry of tree-level amplitudes in $\mathcal{N} = 4$ SYM theory (where $v_j = 0$) this cyclicity is only possible due to the vanishing dual Coxeter number of the underlying Lie algebra $\mathfrak{psu}(2,2|4)$. The above example thus shows that a vanishing dual Coxeter number is not necessary for the existence of cyclic Yangian invariants.

We will now show that Yangian differential equations, similar to (8), also hold for generic fishnet graphs.

SCALAR FISHNETS AND MONODROMY

Generic scalar fishnet graphs (cf. Fig. 1) are composed of the above box diagrams. In order to demonstrate their
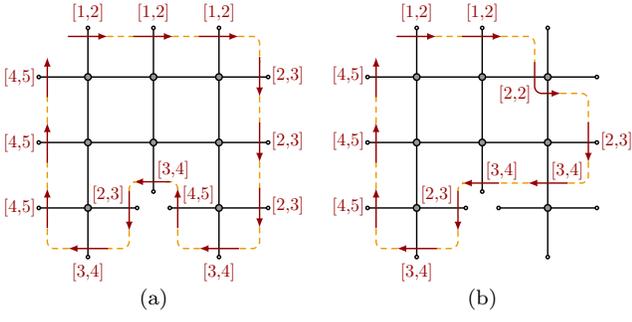
FIG. 3. (a): Monodromy encircling a sample fishnet graph representing the left hand side of (12). (b): Intermediate step of the proof of Yangian symmetry.

FIG. 4. Rules employed to prove the Yangian invariance. (a): The intertwining relation (14). (b) and (c): Pulling the monodromy contour through an integration vertex, cf. (15).

Yangian symmetry, we rephrase the Yangian algebra in terms of the powerful RTT-formulation. Here, the Yangian generators are packaged into a monodromy matrix

$$T(u) \simeq \mathbb{1} + \frac{1}{u} J + \frac{1}{u^2} \widehat{J} + \dots, \tag{9}$$

and the algebra relations are formulated via the Yang–Baxter equation with Yang's R-matrix $R(u) = \mathbb{1} + u\,\mathbb{P}$:

$$R_{12}(u-v)T_1(u)T_2(v) = T_2(v)T_1(u)R_{12}(u-v). \tag{10}$$

We explicitly solve this RTT-relation by defining the monodromy as a product of conformal Lax operators [9]

$$L_{k,\alpha\beta}(u_k^+, u_k^-) = u_k \,\mathbb{1}_{k,\alpha\beta} + \tfrac{1}{2} M_{\alpha\beta}^{ab}\, J_{k,ab}^{\Delta_k}, \tag{11}$$

each of which obeys (10) with $T_k \to L_k$. Here we package the inhomogeneities u_k and the conformal dimensions Δ_k into the symmetric variables $u_k^+ := u_k + \frac{\Delta_k - 4}{2}$ and $u_k^- := u_k - \frac{\Delta_k}{2}$. The $J_{k,ab}$ denote the differential representation of the conformal algebra displayed in (4), and we have $M^{ab} = \frac{i}{4}[\Gamma^a, \Gamma^b]|_{\text{upper block}}$, with Γ^a representing six-dimensional gamma matrices for $\mathbb{R}^{2,4}$. The Yangian symmetry of the box integral I_4 and its n-point generalizations I_n now translates into the eigenvalue equation [10]

$$T(\vec{u})\, I_n = \lambda(\vec{u})\, I_n \,\mathbb{1}, \tag{12}$$

where $T(\vec{u})$ denotes the inhomogeneous monodromy

$$T(\vec{u}) = L_n(u_n^+, u_n^-)L_{n-1}(u_{n-1}^+, u_{n-1}^-)\dots L_1(u_1^+, u_1^-). \tag{13}$$

The choice of parameters $u_k^\pm$ depends on the diagram under consideration. It will be convenient to introduce the notation $[\delta_k^+, \delta_k^-] := (u+\delta_k^+, u+\delta_k^-)$ and $[\delta_k] := u+\delta_k$. By convention we choose the parameters on the boundary legs at the top to be $[1,2]$. Then the parameters on the right, bottom or left boundary legs have to be $[2,3]$, $[3,4]$ or $[4,5]$, respectively (see Fig. 3 for an example). The

Lax operator defined in (11) acts on an auxiliary and a quantum space. While the product in (13) is taken in the auxiliary space, each Lax operator acts on one external leg of the considered graph (the quantum space).

Proving the invariance statement (12) boils down to employing the lasso method [5], i.e. to moving the monodromy through a given graph as displayed in Fig. 3. The most important relation used in this process is the intertwining relation for the Lax operator and the x-space propagator, cf. Fig. 4a:

$$\frac{1}{x_{12}^2} L_2[\delta, \bullet]L_1[\star, \delta+1] = L_2[\delta+1, \bullet]L_1[\star, \delta]\frac{1}{x_{12}^2}. \tag{14}$$

Moreover, we can move a product of Lax operators through an integration vertex via the following relation, cf. Fig. 4b:

$$\int d^4x_0\, L_2[\delta+1, \delta+2]L_1[\delta, \delta+1]\frac{1}{x_{01}^2 x_{02}^2 x_{03}^2 x_{04}^2} \tag{15}$$

$$= [\delta+2] \int d^4x_0\, \frac{1}{x_{01}^2 x_{02}^2} L_0[\delta+1, \delta+1]\frac{1}{x_{03}^2 x_{04}^2}.$$

A third relation of this type is depicted in Fig. 4c. Finally, the Lax operator and its partially integrated version denoted by L^T act on a constant function as

$$L_{\alpha\beta}[\delta, \delta+2] \cdot 1 = L_{\alpha\beta}^T[\delta+2, \delta] \cdot 1 = [\delta+2]\delta_{\alpha\beta}. \tag{16}$$

These rules are sufficient to move the monodromy contour in Fig. 3a through the whole graph to end up with the eigenvalue on the right hand side of (12). See Fig. 3b for an intermediate step. The eigenvalue $\lambda(\vec{u})$ in (12) is composed of the factors picked up in this process via (15) and (16), cf. [5] for explicit expressions.
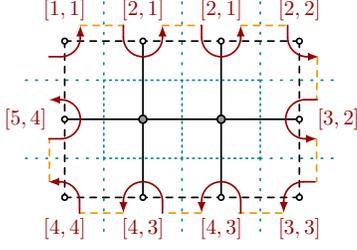
FIG. 5. Double-box integral with massless external legs. Dashed black lines represent delta functions $\delta(x_{i,i+1}^2)$ forcing the momenta (dotted lines) on shell.

OFF- AND ON-SHELL LEGS

Above the external variables x_i^μ were unconstrained. To interpret the x_i as region momenta for a scattering amplitude with massless on-shell legs, we require $p_k^2 = (x_k - x_{k+1})^2 = 0$. Notably, the delta-function imposing this constraint obeys the same intertwining relation as the propagator in (14):

$$\delta(x_{12}^2)\mathrm{L}_2[\delta, \bullet]\mathrm{L}_1[\star, \delta+1] = \mathrm{L}_2[\delta+1, \bullet]\mathrm{L}_1[\star, \delta]\delta(x_{12}^2). \tag{17}$$

We may thus extend the above construction by introducing dashed lines alias delta functions into the graphs, see Fig. 5 for the double-box example. Due to (14) and (17), propagators and delta functions are algebraically interchangeable. Hence, we can set external points (cf. Fig. 5) or internal propagators on shell via insertion of delta functions. Note, however, that the conformal symmetry of massless amplitudes typically shows an anomaly-like behavior for collinear configurations. This can be realized in subtle ways and may require additional contributions to the symmetry generators, cf. e.g. [11–15]. The investigation of this point is in progress.

The generalized boundary configurations as displayed in Fig. 5 require to adapt the inhomogeneities. As can be seen for that example, the conformal dimension $\Delta_k = \delta_k^+ - \delta_k^- + 2$ entering the Lax operator $\mathrm{L}[\delta_k^+, \delta_k^-]$ corresponds to the number of attached propagators, cf. [5].

Notably, the central intertwining relation (14) generalizes to arbitrary powers 2α of the propagator:

$$\frac{1}{x_{12}^{2\alpha}}\mathrm{L}_2[\delta, \bullet]\mathrm{L}_1[\star, \delta+\alpha] = \mathrm{L}_2[\delta+\alpha, \bullet]\mathrm{L}_1[\star, \delta]\frac{1}{x_{12}^{2\alpha}}. \tag{18}$$

This allows us to construct Yangian-invariant deformations of the above correlators and amplitudes. These represent loop-level analogues of the tree-level amplitude deformations found in $\mathcal{N} = 4$ SYM and ABJM theory [16, 17]. Here the powers α_k of propagators entering a vertex obey the conformal constraint $\sum_k \alpha_k = 4$.

The theory defined by (1) is known to generate double-trace interactions $\mathrm{Tr}(\phi_j\phi_j)\mathrm{Tr}(\phi_j^\dagger\phi_j^\dagger)$, $\mathrm{Tr}(\phi_1\phi_2)\mathrm{Tr}(\phi_1^\dagger\phi_2^\dagger)$

and $\mathrm{Tr}(\phi_1\phi_2^\dagger)\mathrm{Tr}(\phi_2\phi_1^\dagger)$ due to quantum corrections [18]. Note that these do not contribute to the correlator (2) at leading order in N_c and hence to the considered planar observables.

INCLUDING FERMIONS

The procedure to obtain integrable quantum field theories as limits of γ-deformed $\mathcal{N} = 4$ SYM theory suggests to consider more general particle species. Adjusting the limit appropriately, one may for instance obtain an interaction Lagrangian including scalars and fermions [3]:

$$\mathcal{L}_{\phi\psi}^{\mathrm{int}} = N_c\mathrm{Tr}\big(\xi_1^2\phi_3^\dagger\phi_1^\dagger\phi^3\phi^1 + \xi_2^2\phi_2^\dagger\phi_1^\dagger\phi^2\phi^1$$
$$+ \sqrt{\xi_1\xi_2}(\bar\psi_1\phi^1\bar\psi_4 - \psi^1\phi_1^\dagger\psi^4)\big). \tag{19}$$

Consider e.g. the following three-loop Feynman graph built from the above Yukawa vertices:
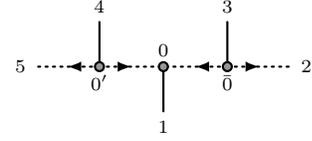
Here dotted lines denote Fermion propagators. The corresponding integral reads

$$I_{\phi\psi} = \int \mathrm{d}^4x_0\mathrm{d}^4x_{\bar 0}\mathrm{d}^4x_{0'}\frac{\overleftarrow{P}_{\mu_2}^{\partial_{\tilde\mu_{\bar 0}}}\vec{P}_{\partial_{\mu_0}}^{\tilde\mu_{\bar 0}}\overleftarrow{P}_{\mu_0}^{\partial_{0'}}\vec{P}_{\mu_5}^{\tilde\mu_{0'}}}{x_{10}^2x_{3\bar0}^2x_{40'}^2}, \tag{20}$$

where the Fermion propagators are expressed using the notation

$$\overleftarrow{P}_{A_1}^{A_2} = \frac{\langle A_1|x_{12}|A_2]}{x_{12}^4}, \qquad \vec{P}_{A_1}^{A_2} = \frac{[A_2|x_{12}|A_1\rangle}{x_{12}^4}. \tag{21}$$

We employ dummy $\mathfrak{su}(2)$ spinors with brackets $\langle\mu|$ and $[\tilde\mu|$, respectively, in order to avoid explicit indices. Notably, also the propagators (21) obey intertwining relations including Lax operators L^{f} and $\mathrm{L}^{\bar{\mathrm{f}}}$ in the $(\frac{1}{2}, 0)$ and $(0, \frac{1}{2})$ representations of the Lorentz group, respectively, for instance

$$\mathrm{L}_2^{\mathrm{f}}(u + \tfrac{3}{2}, \bullet)\mathrm{L}_1(\star, u)\overleftarrow{P}_{\mu_2}^{\partial_{\tilde\mu_1}} = \overleftarrow{P}_{\mu_2}^{\partial_{\tilde\mu_1}}\mathrm{L}_2(u, \bullet)\mathrm{L}_1^{\bar{\mathrm{f}}}(\star, u + \tfrac{3}{2}). \tag{22}$$

Here the operators L^{f} and $\mathrm{L}^{\bar{\mathrm{f}}}$ are defined via (11), but now with non-zero spin matrices S in (4). Acting on the above spinors, we have $S_{\rho\sigma}^{\mathrm{f}} = \mu \cdot \sigma_{\rho\sigma}^+ \cdot \partial_\mu$ and $S_{\rho\sigma}^{\bar{\mathrm{f}}} = \tilde\mu \cdot \sigma_{\rho\sigma}^- \cdot \partial_{\tilde\mu}$, where $\sigma_{\rho\sigma}^\pm = \frac{i}{4}(\sigma_\rho^\pm\sigma_\sigma^\mp - \sigma_\sigma^\pm\sigma_\rho^\mp)$ and $\sigma_\mu^\pm = (\sigma_0, \pm\sigma_1, \pm\sigma_2, \pm\sigma_3)_\mu$; for more details see [6, 9]. Also in this case proving the Yangian invariance boils down to pulling the monodromy through propagators and vertices. The fermionic Lax operators are not proportional to the identity when acting on a constant (cf. (16) for the scalar case) but cancel via $\mathrm{L}^{\bar{\mathrm{f}}}\mathrm{L}^{\mathrm{f}}P \sim P$ on the propagator P.

If we consider the model (19) and an amplitude that describes the scattering of both types of fermions and only the boson ϕ^1, this scattering process corresponds to a single "brick wall" Feynman graph, whose bulk structure is given by a regular fishnet lattice consisting of only Yukawa vertices, e.g.
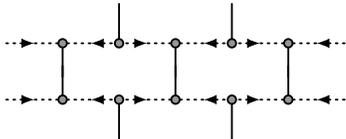
This type of integrable fishnet is new with respect to the examples given in [1]. If we also include the other two types of bosons of (19), each color-ordered amplitude is represented by a single Yangian-invariant graph with a mixture of rectangular and hexagonal fishnet structures.

THREE AND SIX DIMENSIONS

Instead of considering the parameter α in (18) as a deformation in $4d$, we may associate it with the space-time dimension d via $\alpha = \frac{d-2}{2}$ and replace the four-dimensional Lax operators L_k by an appropriate d-dimensional counterpart L_k^d, cf. [6]. Then the above off-shell construction generalizes to the cases of amplitudes in $d = 3$ and $d = 6$ spacetime dimensions built from scalar six- and three-point vertices, respectively. The above action of the scalar Lax operator on the vacuum (16) becomes

$$\mathrm{L}_{\alpha\beta}^d[\delta, \delta + \tfrac{d}{2}] \cdot 1 = \mathrm{L}_{\alpha\beta}^{d\,T}[\delta + \tfrac{d}{2}, \delta] \cdot 1 = [\delta + \tfrac{d}{2}]\delta_{\alpha\beta}. \quad (23)$$

For $d = 3$ and $d = 6$ the scalar graphs form triangular and hexagonal fishnets, respectively. These complete the set of regular tilings of the plane—all furnishing Yangian-invariant scalar Feynman diagrams, cf. Tab. I. Corresponding field theories were recently proposed in [3, 19]. While the three-dimensional triangle graphs arise from scalar limits of planar, γ-deformed ABJM theory [3], a six-dimensional "mother" theory is not known.

Due to the dimensionality of the propagators, in three and six dimensions we cannot use the naive trick to replace the propagator by a delta function $\delta(x_{ij}^2)$ in order to go on shell, cf. Tab. I and (17). It is possible, however, to set up a momentum space Lax formalism to show the Yangian invariance of on-shell graphs [6].

CONCLUSIONS AND OUTLOOK

The Yangian algebra underlies the Bethe ansatz and the quantum inverse scattering method. Its finding in the present context gives hope for the applicability of similar solution techniques to the largely unsolved class of fishnet integrals (cf. [20] in this context [21]). In four

Dimension	$d = 3$	$d = 4$	$d = 6$
Propagator	$\lvert x_{ij}\rvert^{-1}$	$\lvert x_{ij}\rvert^{-2}$	$\lvert x_{ij}\rvert^{-4}$
Scalar Fishnet			

TABLE I. Overview of scalar fishnet graphs.

dimensions merely the box integral is solved [8] and already the double box is expected to yield complicated elliptic functions [22]. This renders new insights into the mathematical structure of fishnet integrals valuable.

The above classes of Feynman graphs define specific double scaling limits of scattering amplitudes in planar γ-deformed $\mathcal{N} = 4$ SYM and ABJM theory. This suggests a set of non-trivial, integrable and non-supersymmetric CFTs in four dimensions, whose existence puts understanding the origins of integrability of the respective "mother" theories within reach. This finding is also remarkable since the study of symmetry-invariant subsectors has been crucial for developing the powerful integrability tools for the spectrum of AdS/CFT. In particular, our results show that cyclic Yangian-invariant scattering amplitudes exist even if the dual Coxeter number of the underlying symmetry algebra does not vanish, i.e. for cases different from the full $\mathcal{N} = 4$ SYM or ABJM theory.

A further important goal is to establish the Yangian symmetry for the most general double-scaled model of [2], containing three couplings, three bosons and three fermions.

―――――

* chicherin@uni-mainz.de
† kazakov@physique.ens.fr
‡ loebbert@physik.hu-berlin.de
§ dmueller@physik.hu-berlin.de
¶ zdlzdlzdl@gmail.com

[1] A. B. Zamolodchikov, Phys. Lett. **B97**, 63 (1980).
[2] O. Gurdogan and V. Kazakov, (2015), arXiv:1512.06704 [hep-th].
[3] J. Caetano, O. Gurdogan, and V. Kazakov, (2016), arXiv:1612.05895 [hep-th].
[4] N. Gromov, V. Kazakov, G. Korchemsky, S. Negro, and G. Sizov, arXiv:1706.04167 [hep-th].

[5] D. Chicherin, V. Kazakov, F. Loebbert, D. Müller, and D.-l. Zhong, (2017), arXiv:1704.01967 [hep-th].

[6] D. Chicherin, V. Kazakov, F. Loebbert, D. Müller, and D.-l. Zhong, "In preparation." (2017).

[7] Here we do not discuss the even simpler tree-level diagrams. See [5] for comments.

[8] N. Ussyukina and A. I. Davydychev, Physics Letters B **298**, 363 (1993).

[9] D. Chicherin, S. Derkachov, and A. P. Isaev, JHEP **04**, 020 (2013), arXiv:1206.4150 [math-ph].

[10] D. Chicherin and R. Kirschner, Nucl. Phys. **B877**, 484 (2013), arXiv:1306.0711 [math-ph].

[11] T. Bargheer, N. Beisert, W. Galleas, F. Loebbert, and T. McLoughlin, JHEP **11**, 056 (2009), arXiv:0905.3738 [hep-th].

[12] A. Sever and P. Vieira, (2009), arXiv:0908.2437 [hep-th].

[13] N. Beisert, J. Henn, T. McLoughlin, and J. Plefka, JHEP **04**, 085 (2010), arXiv:1002.1733 [hep-th].

[14] S. Caron-Huot and S. He, JHEP **07**, 174 (2012), arXiv:1112.1060 [hep-th].

[15] T. Bargheer, N. Beisert, F. Loebbert, and T. McLoughlin, J. Phys. **A45**, 475402 (2012), arXiv:1204.4406 [hep-th].

[16] L. Ferro, T. Lukowski, C. Meneghelli, J. Plefka, and M. Staudacher, Phys. Rev. Lett. **110**, 121602 (2013), arXiv:1212.0850 [hep-th].

[17] T. Bargheer, Y.-t. Huang, F. Loebbert, and M. Yamazaki, Phys. Rev. **D91**, 026004 (2015), arXiv:1407.4449 [hep-th].

[18] C. Sieg and M. Wilhelm, Phys. Lett. **B756**, 118 (2016), arXiv:1602.05817 [hep-th].

[19] O. Mamroud and G. Torrents, (2017), arXiv:1703.04152 [hep-th].

[20] B. Basso and L. J. Dixon, (2017), arXiv:1705.03545 [hep-th].

[21] Our method to prove Yangian invariance does not immediately apply to the graphs considered in [20]. Their coincidence limit of external points annihilates some degrees of freedom.

[22] S. Caron-Huot and K. J. Larsen, JHEP **10**, 026 (2012), arXiv:1205.0801 [hep-ph].